Implementation of a Multisegmented, Quasi-Static Cable Model

Preprint

M. Masciola, J. Jonkman, and A. Robertson
National Renewable Energy Laboratory

To be presented at the 23rd International Ocean (Offshore) and Polar Engineering Conference
Anchorage, Alaska
June 30-July 5, 2013

NREL is a national laboratory of the U.S. Department of Energy, Office of Energy Efficiency & Renewable Energy, operated by the Alliance for Sustainable Energy, LLC.

Conference Paper
NREL/CP-5000-57812
March 2013

Contract No. DE-AC36-08GO28308

Available electronically at http://www.osti.gov/bridge

Available for a processing fee to U.S. Department of Energy
and its contractors, in paper, from:

U.S. Department of Energy
Office of Scientific and Technical Information
P.O. Box 62
Oak Ridge, TN 37831-0062
phone: 865.576.8401
fax: 865.576.5728
email: mailto:reports@adonis.osti.gov

Available for sale to the public, in paper, from:

U.S. Department of Commerce
National Technical Information Service
5285 Port Royal Road
Springfield, VA 22161
phone: 800.553.6847
fax: 703.605.6900
email: orders@ntis.fedworld.gov
online ordering: http://www.ntis.gov/help/ordermethods.aspx

Cover Photos: (left to right) PIX 16416, PIX 17423, PIX 16560, PIX 17613, PIX 17436, PIX 17721

Printed on paper containing at least 50% wastepaper, including 10% post consumer waste.

Implementation of a Multisegmented, Quasi-Static Cable Model

Marco Masciola, Jason Jonkman, and Amy Robertson
National Renewable Energy Laboratory
Golden, CO USA

ABSTRACT

The Mooring Analysis Program (MAP) is a library designed to be used in parallel with other computer-aided engineering (CAE) tools to model the static and dynamic forces of mooring systems. In this paper, the implementation of a multisegmented, quasi-static (MSQS) mooring model in MAP is investigated. The MSQS model was developed based on an extension of conventional single-line static solutions. Conceptually, the MSQS program simultaneously solves the algebraic equations for all elements with the condition that the total force at connection points sum to zero. Seabed contact, seabed friction, and externally applied forces can be modeled with this tool, and it allows multielement mooring systems with arbitrary connection configurations to be analyzed. This paper provides an introduction to MAP's MSQS model, its underlying theory, and a demonstration of its abilities.

KEY WORDS: Quasi-static mooring; catenary; cable simulation

NOMENCLATURE

B	Buoyancy tank
EA	Mooring line axial stiffness
C_B	Cable-seabed friction coefficient
$F_{X,Y,Z}$	X, Y, and Z global forces
H, H_A	Horizontal force at the fairlead and anchor
h, l	Horizontal and vertical cable excursion
L	Unstretched cable length
M	Point mass
V, V_A	Vertical force at the fairlead and anchor
$T_e(s)$	Line tension at s
W	Cable weight per unit length
x_i, z_i	Local (element) coordinates
X_i, Y_i, Z_i	Global coordinates

INTRODUCTION

The Mooring Analysis Program (MAP) is an open-source project being developed by the National Renewable Energy Laboratory (NREL) to support the modeling of floating offshore wind turbines, wave energy converters, ocean current turbines, and related research topics. Since MAP is intended for use across a wide range of applications, thoughtful consideration must be made regarding the user interface, inputs, outputs, and access points for other programs to call the MAP library. With support from the U.S. Department of Energy (DOE), NREL developed a modularization framework for the wind turbine simulation program FAST (Jonkman and Buhl, 2005). This framework was created to enable developers to seamlessly integrate customized modules into FAST while preserving the integrity of the numerical simulation (Jonkman, 2013). MAP adheres to this framework and function-call convention. Because MAP is designed as a library, critical functions are exposed to outside programs, allowing other simulation tools to dynamically link with MAP in the same way that FAST would.

The multisegmented, quasi-static (MSQS) component of MAP was developed to meet the need for a tool that could model the nonlinear stiffness matrix and static forces of practical mooring systems with arbitrary connection geometries and profiles. The quasi-static model used in MAP was derived from a set of closed-form analytical solutions of a continuous cable with homogeneous properties (Irvine, 1992). Such models account for the effects of distributed cable mass, strain, and cable elasticity to provide the line profile and effective forces for a cable suspended at steady-state (static equilibrium). Forces arising from inertia, viscous drag, internal damping, bending, and torsion are neglected. Still, the quasi-static representation is a reasonable approximation to the mooring line restoring forces in lieu of comprehensive finite-element analysis (FEA) models (API, 1997).

The theory behind single-line quasi-static mooring representations is sufficiently described in existing literature (Irvine, 1992; Wilson, 2003). Although these models have widespread utility (Kozak, *et al*, 2006; Paul and Soler, 1995; Wang, *et al*, 2010), the representations cited are limited to single-line mooring elements, Fig. 1(a). In marine applications, a spread mooring with a bridle connection is adopted in most mooring designs, Fig. 1(b). This configuration provides lateral stiffness in the Y direction that otherwise would not be present with a single-line. Peyrot and Goulois (1979) demonstrated a solution to the multisegmented cable, which a bulk of this work is based on. The current MSQS model, however, refines the program architecture to solve a wide range of problems with unknowns and arbitrary geometries defined at run-time. A unique feature of the quasi-static model presented in this paper is the inclusion of seabed contact forces in the formulation. In the present mooring line implementation in FAST, only single-line elements, such as the one depicted in Fig. 1(a), are solvable. The multiline representation depicted in Fig. 1(b) can be solved with MAP's MSQS model. The MSQS model provides a foundation for the development of a mooring line program with dynamic capabilities, such as a lumped mass model, FEA, or finite differencing models.

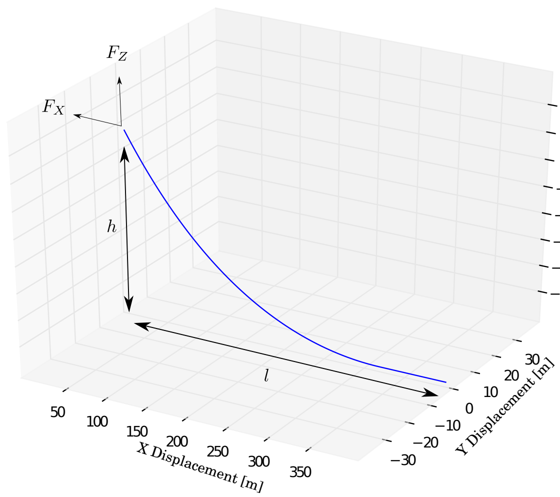

(a)

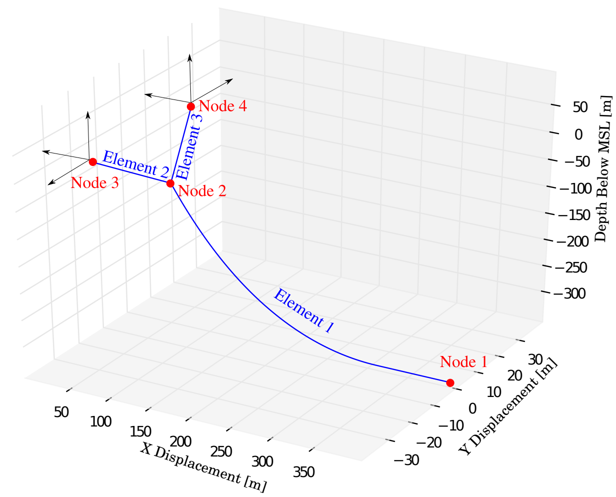

(b)

Fig. 1: In (a), the mooring line is modeled as a single-line element; hence, the resulting restoring force supplied to the platform is restricted to the plane of the mooring line. In contrast, a multisegmented line can model a fairlead force with components in the X, Y, and Z directions, (b).

Manuscript Objective

The focus of this paper is to present features of the MSQS model and to conduct validation checks on basic mooring geometries. The theory is presented to help readers understand the type of problems that the MSQS model can handle. This paper briefly describes the program user interface and input options. For greater details on the function-calling convention, Python interface, and recommendations on how to couple MAP with other codes, refer to the MAP user manual (Masciola and Jonkman, forthcoming)[1].

Abilities of the MSQS Model

The MSQS model is developed without imposing boundary condition rules. In some cases, the user may choose to partially specify boundary conditions to inverse design a mooring system to meet specific design requirements. For instance, consider the conceptual problem of an underwater ocean current turbine where the thrust force generated by the rotating blades is known. The mooring is anchored at its bottom end at a known point and the fairlead is free to slide at height h in the horizontal direction. Using Fig. 1(a) to illustrate this problem, a known horizontal force F_X is applied at the fairlead. The variables solved in this case would be the F_Z fairlead force and the horizontal cable excursion l away from the anchor point. This approach departs from traditional quasi-static implementations used in dynamics simulations, where the forces applied at the fairleads are solved based on the mooring line displacement values (h and l). Note that MAP allows an external force $F^{ext}_{X,Y,Z}$, node mass M, and volumetric displacement B to be specified at each node. These features give the MSQS model the flexibility to function as a design tool or a simulation model.

Although MAP's native language is `C++`, the program is constructed with wrappers, allowing users to dynamically interact with MAP in Python (Langtangen, 2011). This gives users the flexibility to call the MAP program functions, create and initialize data structures, pass data to the MAP solvers, perform checks on the model inputs, and plot mooring line profiles from Python. The core program solvers, solution strategy, procedures, and functions remain in `C++`. MAP is compiled with the Portable, Extensible Toolkit for Scientific Computation (PETSc) open-source numerical library to include a Scalable Nonlinear Equations Solver (SNES) package suitable for solving ill-conditioned problems that commonly arise in multisegmented models (Balay, *et al*, 2012). The PETSc package provides a variety of nonlinear solver strategies, including a trust region and a Newton linear search method (Faires and Burden, 2003), that are all enabled/disabled at run-time. The solver tolerance and other options can be set at run-time through the MAP input text file.

[1]http://wind.nrel.gov/designcodes/simulators/map/

MULTISEGMENTED, QUASI-STATIC THEORY

MAP's MSQS model is developed as an extension of a single-line element theory combining several individual catenary cables at common connection points. Once combined, static equilibrium is achieved when the connection point forces sum to zero. This scheme requires two different sets of equations to be solved. The first is the continuous catenary algebraic equations (Irvine, 1992). The second equation resolves the sum forces at the connection points to check if equilibrium is reached.

A detail that must be addressed is transforming the conventional two-dimensional catenary equations into a three-dimensional domain to resolve the Newton force-balance equation at each connection node. Two equations are sufficient to describe the profile of a catenary cable because each element lies in one plane, Fig. 1(a). For generality, the assembled multisegmented line is modeled as a three-dimensional system. In this section, the composition of the equations solved and system kinematics of the multisegmented cable are explored.

Catenary Equation for a Single-Line

The solution to the common closed-form analytical equation for a single-line cable element hanging between two fixed points was derived independently in numerous works (Irvine, 1981; Wilson, 2003):

$$x\left(s\right) = \frac{H}{W}\left[\sinh^{-1}\left(\frac{V_A + Ws}{H}\right) - \sinh^{-1}\left(\frac{V_A}{H}\right)\right] + \frac{Hs}{EA} \quad (1a)$$

$$z(s) = \frac{H}{W}\left[\sqrt{1+\left(\frac{V_A+Ws}{H}\right)^2} - \sqrt{1+\left(\frac{V_A}{H}\right)^2}\right] + \frac{1}{EA}\left(V_A s + \frac{Ws^2}{2}\right) \tag{1b}$$

where x and z are coordinates relative to the element frame, Fig. 2. By recognizing that the vertical force changes proportionately with the cable mass density, and that external horizontal forces are absent on the cable between the anchor and fairlead, the following conditions hold:

$$H_A = H \tag{2a}$$

$$V_A = V - WL \tag{2b}$$

The horizontal l and vertical h fairlead displacement can be found by substituting $s = L$ in Eqs. 1a∼1b to yield:

$$l = \frac{H}{W}\left[\sinh^{-1}\left(\frac{V}{H}\right) - \sinh^{-1}\left(\frac{V-WL}{H}\right)\right] + \frac{HL}{EA} \tag{3a}$$

$$h = \frac{H}{W}\left[\sqrt{1+\left(\frac{V}{H}\right)^2} - \sqrt{1+\left(\frac{V-WL}{H}\right)^2}\right] + \frac{1}{EA}\left(VL - \frac{WL^2}{2}\right) \tag{3b}$$

The tension at any point in the mooring is:

$$T_e(s) = \sqrt{H^2 + (V_A + Ws)^2} \tag{4}$$

These equations are valid for a hanging cable that is not in contact with the seabed, and the mooring is guaranteed to be suspended (and not in contact with the seabed), provided that the vertical fairlead force is greater than the weight of the mooring. Therefore, the above equations apply if the following sufficient, but not necessary, condition is met:

$$(V - WL) > 0 \tag{5}$$

Likewise, a mooring line will remain suspended in the water column if the net mooring weight in the fluid is less than zero.

Catenary in Contact with the Seabed

If the vertical force V is less than the total weight of the cable (i.e., $V \leq WL$), then a portion of the mooring line will rest on the seabed and the conditions in Eq. 5 will be violated. The unstretched length of cable lying on the seabed can be found from $L_B = L - \frac{V}{W}$ (Jonkman, 2007), where L_B is assumed positive. When $L_B > 0$, the formulation of Eqs. 3a∼3b change because the following must now be accounted for: a) seabed friction in the horizontal direction, and b) a decrease in the vertical force V proportional to the length of cable lying on the seabed. This leads to the following modifications of Eqs. 1a∼1b (Jonkman, 2007):

$$x(s) = \begin{cases} s & \text{for } 0 \leq s \leq \gamma \\ s + \frac{C_B W}{2EA}\left[s^2 - 2s\gamma + \gamma\lambda\right] & \text{for } \gamma \leq s \leq L_B \\ L_B + \frac{H}{W}\sinh^{-1}\left[\frac{W(s-L_B)}{H}\right] & \text{for } L_B \leq s \leq L \\ +\frac{Hs}{EA} + \frac{C_B W}{2EA}\left[\lambda\gamma - L_B^2\right] & \end{cases} \tag{6a}$$

$$z(s) = \begin{cases} 0 & \text{for } 0 \leq s \leq L_B \\ \frac{H}{W}\left[\sqrt{1+\left(\frac{W(s-L_B)}{H}\right)^2} - 1\right] & \text{for } 0 \leq s \leq L \\ +\frac{W(s-L_B)^2}{2EA} & \end{cases} \tag{6b}$$

with $\gamma = L_B - \frac{H}{C_B W}$ and

$$\lambda = \begin{cases} \gamma & \text{if } \gamma > 0 \\ 0 & \text{otherwise} \end{cases} \tag{7}$$

Substituting $s = L$ into Eqs. 6a∼6b yields the vertical and horizontal extension limits of the mooring line:

$$l = L_B + \frac{H}{W}\sinh^{-1}\left(\frac{V}{H}\right) + \frac{HL}{EA} + \frac{C_B W}{2EA}\left[\mu\left(L - \frac{V}{W} - \frac{H}{C_B W}\right) - \left(L - \frac{V}{W}\right)^2\right] \tag{8a}$$

$$h = \frac{H}{W}\left[\sqrt{1+\left(\frac{V}{H}\right)^2} - 1\right] + \frac{V^2}{2EAW} \tag{8b}$$

where the parameter μ is sought from:

$$\mu = \begin{cases} L - \frac{V}{W} - \frac{H}{C_B W} & \text{if } \left(L - \frac{V}{W} - \frac{H}{C_B W}\right) > 0 \\ 0 & \text{otherwise} \end{cases} \tag{9}$$

The line tension as a function of unstretched payout s is given by:

$$T_e(s) = \begin{cases} \max\left[H + C_B W(s - L_B)\ ,\ 0\right] & \text{for } 0 \leq s \leq L_B \\ \sqrt{H^2 + \left[W(s - L_B)\right]^2} & \text{for } L_B < s \leq L \end{cases} \tag{10}$$

Line Kinematics

A vector breakdown of Fig. 1(b) is given in Fig. 3 to illustrate the kinematic entities in transforming a two-dimensional line into a three-dimensional representation. Vector $\mathbf{r}_i$ denotes the position of frame $\mathcal{F}_i$, with respect to the XYZ axis. In the local $\mathcal{F}_i$ frame, vector:

$$\mathbf{q}_i(s) = \left[x_i(s)\ ,\ 0\ ,\ z_i(s)\right]^T \tag{11}$$

represents the displacement vector from the origin of $\mathcal{F}_i$ to points tangent to the line. When $s = L$, then $\mathbf{q}_i(s = L) = \left[l_i\ ,\ 0\ ,\ h_i\right]^T$, which describes the displacement vector from anchor to fairlead. The components of $l_i(s)/h_i(s)$ are determined from Eqs. 3a∼3b or Eqs. 8a∼8b, depending on whether the line is suspended or in contact with the ground. The orientation of the local frame $\mathcal{F}_i$ relative to the global $\mathcal{F}_0$ frame is:

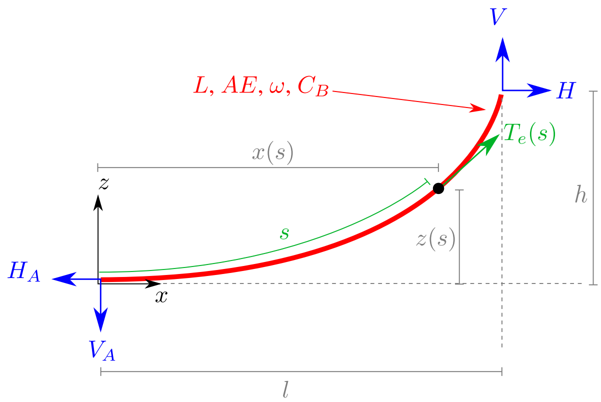

Fig. 2: Definition of the entities in a single-line mooring line relative to the local xz axis.

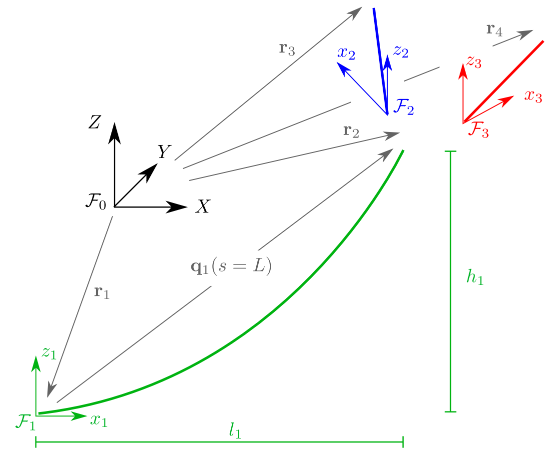

Fig. 3: Notation of the various entities needed in defining the relationship between multiple members in a multisegmented mooring line.

$$\begin{aligned}\psi_i &= \cos^{-1}\left\{\frac{\left(\{\mathbf{r}_j\}^{x,y} - \{\mathbf{r}_i\}^{x,y}\right)\cdot\hat{\mathbf{i}}}{\|\{\mathbf{r}_j\}^{x,y} - \{\mathbf{r}_i\}^{x,y}\|}\right\} \\ &= \cos^{-1}\left\{\frac{\{\mathbf{r}_j\}^{x} - \{\mathbf{r}_i\}^{x}}{\sqrt{\left(\{\mathbf{r}_j\}^{x} - \{\mathbf{r}_i\}^{x}\right)^2 + \left(\{\mathbf{r}_j\}^{y} - \{\mathbf{r}_i\}^{y}\right)^2}}\right\}\end{aligned} \tag{12}$$

where ψ_i is indicative of a rotation about the global Z axis, $\{\mathbf{r}_j\}^{x,y}$ is the presumed mooring line anchor point (i.e., the origin of $\mathcal{F}_i$), $\mathbf{r}_j$ is the upper node (fairlead) position, and $\hat{\mathbf{i}} = [1\ ,\ 0\ ,\ 0]^T$ is a unit vector aligned with the X axis. Note that for all line elements, z_i is always parallel to Z; so a single rotation about Z is sufficient to describe the orientation of all elements. Only the x and y components of $\mathbf{r}_{i,j}$ are needed to compute ψ in Eq. 12. The profile for a mooring line can then be obtained in the XYZ frame with:

$$\mathbf{X}_i(s) = \mathbf{r}_i + \mathbf{R}_i\mathbf{q}_i(s) \tag{13}$$

where the transformation from frame $\mathcal{F}_i$ into $\mathcal{F}_0$ is done using the following orthogonal matrix:

$$\mathbf{R}_i = \begin{bmatrix}\cos\psi_i & -\sin\psi_i & 0 \\ \sin\psi_i & \cos\psi_i & 0 \\ 0 & 0 & 1\end{bmatrix} \tag{14}$$

After substituting Eq. 11 and Eq. 14 into Eq. 13, the following is obtained:

$$\mathbf{X}_i(s) = \mathbf{r}_i + \left[x_i(s)\cos\psi_i\ ,\ x_i(s)\sin\psi_i\ ,\ z_i(s)\right]^T \tag{15}$$

Solving the MSQS Model

The solution process begins by evaluating the two continuous analytical catenary equations for each element based on l and h values obtained through node displacement relationships. An element is defined as the component connecting two adjacent nodes together. Once the element fairlead (H, V) and anchor (H_A, V_A) forces are solved at the element level, the forces are transformed from the local $x_i z_i$ frame into the global XYZ coordinate system. The force contribution at each element's anchor and fairlead is added to the corresponding node it attaches to. The force-balance equation is evaluated for each node, as follows:

$$\{\mathbf{F}\}_X^j = \sum_{i=1}^{\text{Elements } i \text{ at Node } j} \left[H_i\cos(\psi_i)\right] - F_X^{ext} \leq \epsilon \tag{16a}$$

$$\{\mathbf{F}\}_Y^j = \sum_{i=1}^{\text{Elements } i \text{ at Node } j} \left[H_i\sin(\psi_i)\right] - F_Y^{ext} \leq \epsilon \tag{16b}$$

$$\{\mathbf{F}\}_Z^j = \sum_{i=1}^{\text{Elements } i \text{ at Node } j} \left[V_i\right] - F_Z^{ext} + Mg - \rho g B \leq \epsilon \tag{16c}$$

where ϵ is the convergence tolerance limit. Based on the error of Eqs. 16a∼16c, the node position is updated. As an outcome, the element forces must be recalculated, and the process begins again. Clearly, this process requires two distinct sets of equations to be simultaneously solved to achieve the static cable configuration. The first set of equations are the force-balance relationships in three directions for each node; the second set of equations are the two catenary functions. The nested solver procedure is summarized by the following sequence of events:

1) The problem is initialized to the extent that elements (and their properties) are defined, associations between elements and nodes are established, and user-supplied boundary conditions are declared for the model. Each node in the array is given a classification to determine if a Newton force-balance calculation is needed.
2) $\mathbf{x}_0$ is set. The guess $\mathbf{x}_0$ defines initial estimates for each node variable being solved.
3) $\mathbf{y}_0$ is set. The guess $\mathbf{y}_0$ defines initial estimates for each element variable being solved.
4) The outer-loop iteration begins. The outer-loop step uses the initial state vector $\mathbf{x}_0$ to iterate the element properties.
    a) The inner-loop iteration begins. The purpose of the inner-loop iteration is to use the continuous cable equation to solve for the unknown quantities, Eqs. 3a∼3b or Eqs. 8a∼8b.
    b) Based on the current state vector $\mathbf{x}_0$ value and element initial guess $\mathbf{y}_0$, the unknown components in the element state vector are solved.
    c) The node initial guess vector $\mathbf{y}_0$ is updated with $\mathbf{y}_1$.

d) Once the unknowns are solved, the anchor and fairlead forces are passed to their respective attaching nodes and summed to find the total force. This concludes the inner-loop solver.

5) The force balance equation is evaluated for each nonfixed node.
6) The node initial guess vector $\mathbf{x}_0$ is updated with $\mathbf{x}_1$.
7) Steps 4–6 are repeated until the following objective $\sum \mathbf{F} \leq \epsilon$ is achieved for Eqs. 16a∼16c.

THE MAP INPUT FILE

The model input mechanism for MAP is an ASCII-based text file as shown in Fig. 4 (as an example). Values prefixed by '#' are used to identify variables iterated by the numerical solver, with the value supplied as the initial guess. The initial guess value can be absent. Not all values in the MAP input file can be iterated, and the particular solvable entries are limited to those contained in the `NODE PROPERTIES` and `LINE PROPERTIES` portion of the MAP input file. MAP will alert users if the number of iterated variables exceeds the number of algebraic equations that can be solved. This paper provides a topical discussion on the input file format; consult Masciola and Jonkman (forthcoming) for a more detailed description of the input file requirements. There are four sections to the MAP input file, as shown in Fig. 4:

- `LINE DICTIONARY`: This section defines the line properties, such as the line diameter, elastic properties, and material density.
- `NODE PROPERTIES`: Nodes are used to define the element fairlead and anchor displacements. The application point of fairlead and anchor forces occur at nodes. External forces, such as buoyancy, weight, or thrust, can be applied to the node using the `M`, `B`, `FX`, `FY`, and `FZ` options.
- `LINE PROPERTIES`: Each line has characteristics defined in the `LINE DICTIONARY` section that allow users to select unique lengths for each element. Integer values are used to link the corresponding nodes that act as fairlead and anchor points.
- `SOLVER OPTIONS`: The PETSc numerical library has an extensive list of options available to solve nonlinear systems. Rather than setting these options at compile-time, the user can set tolerances, solver strategies, and matrix preconditioners at run-time (Balay, *et al*, 2012).

Element run-time options are set using the `Flags` tag. For the case specified in Fig. 4, the option to plot the cable profile for all three elements is selected. In this example, the input file illustrates a desire to solve the mooring system depicted in Fig. 1(b) with a predefined vertical force of $V = 500000$ N applied to node 3 and 4, but an undetermined length of line for elements 2 and 3. The total force applied to node 2 (the node binding the three elements together) must sum to zero in the three directions, so its XYZ displacement is solved. The numerical values following a '#' symbol are indicative of a user-supplied initial guess. At the element level, the unstretched lengths for elements 2 and 3 are iterated, as identified by the flag preceding `UnstrLen`. The cable weight per unit length is calculated using:

$$W = gA\left(\texttt{RhoInAir} - \rho_{\text{water}}\right) \tag{17}$$

where $A = \pi \frac{\texttt{Diam}^2}{4}$. The unknowns listed in the MAP input file in Fig. 4 are solved with the following solution achieved at convergence:

- Node 1: $F_X = 158079$ N, $F_Y = 0$ N, $F_Z = 0$ N
- Node 2: $X = 64.012$ m, $Y = 0.000$ m, $Z = -115.425$ m
- Node 3: $F_X = -202389$ N, $F_Y = 91970$ N
- Node 4: $F_X = -202389$ N, $F_Y = -91970$ N
- Element 2 & 3: $L = 115.9$ m

```
--------------- LINE DICTIONARY -------------------------
LineType  Diam  RhoInAir  E        CB
(-)       (m)   (kg/m^3)  (N/m^2)  (-)
steel     0.25  6500      200E9    1.0
nylon     0.30  1400      14E9     1.0
--------------- NODE PROPERTIES -------------------------
Node  Type      X     Y    Z     M    B     FX   FY  FZ
(-)   (-)      (m)   (m)  (m)   (kg) (m^3)  (N)  (N) (N)
1     Fix      400   0    -350  0    0      #    #    #
2     Connect  #90   #0   #-80  0    0      0    0    0
3     Vessel   20    20   -10   0    0      #    #    500000
4     Vessel   20   -20   -10   0    0      #    #    500000
--------------- LINE PROPERTIES -------------------------
Element  LineType  UnstrLen   NodeAnch  NodeFair  Flags
(-)      (-)       (m)        (-)       (-)       (-)
1        steel     450        1         2         plot
2        nylon     #90        2         3         plot
3        nylon     #90        2         4         plot
--------------- SOLVER OPTIONS---------------------------
(-)
-snes_type tr
-snes_max_it 500
-pc_type svd
-ksp_type tfqmr
-snes_atol 1e-6
-snes_rtol 1e-6
-snes_stol 1e-6
```

Fig. 4: The parameters specified in this MAP input file are consistent with the mooring profile illustrated in Fig. 1(b).

```
--------------- LINE DICTIONARY -----------------------
LineType Diam RhoInAir E       CB
(-)      (m)  (kg/m^3) (N/m 2) (-)
steel    0.25 7000     200E9   1.0
--------------- NODE PROPERTIES -----------------------
Node Type     X     Y    Z      M    B     FX   FY   FZ
(-)  (-)      (m)   (m)  (m)    (kg) (m^3) (N)  (N)  (N)
1    fix      325   0    -350   0    0     #    #    #
2    connect  #288  #0   #-311  0    0     0    0    0
3    connect  #252  #0   #-272  0    0     0    0    0
4    connect  #216  #0   #-233  0    0     0    0    0
5    connect  #180  #0   #-194  0    0     0    0    0
6    connect  #144  #0   #-155  0    0     0    0    0
7    connect  #108  #0   #-116  0    0     0    0    0
8    connect  #72   #0   #-77   0    0     0    0    0
9    connect  #36   #0   #-38   0    0     0    0    0
10   fix      0     0    0      0    0     #    #    #
--------------- LINE PROPERTIES -----------------------
Element LineType UnstrLen NodeAnch NodeFair Flags
(-)     (-)      (m)      (-)      (-)      (-)
1       steel    55.55    1        2    x_force z_force
2       steel    55.55    2        3    x_force z_force
3       steel    55.55    3        4    x_force z_force
4       steel    55.55    4        5    x_force z_force
5       steel    55.55    5        6    x_force z_force
6       steel    55.55    6        7    x_force z_force
7       steel    55.55    7        8    x_force z_force
8       steel    55.55    8        9    x_force z_force
9       steel    55.60    9        10   x_force z_force
--------------- SOLVER OPTIONS-------------------------
Option
(-)
-snes_type ls
-snes_max_it 500
-pc_type svd
-ksp_type gmres
-snes_atol 1e-6
-snes_rtol 1e-6
-snes_stol 1e-6
```

Fig. 5: Input deck for a multisegmented, single-line system. The line is suspended between $l = 325$ and $h = -350$ meters. The element option flags `x_force` and `z_force` will output the X and Z fairlead force relative to the global reference frame. The `X` and `Z` displacements for the in-between nodes are estimated to be evenly separated between $0 - 325$ m and $0 - 350$ m, respectively.

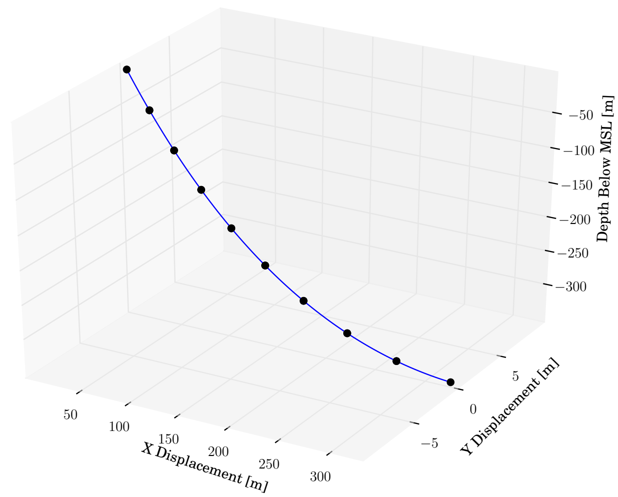

Fig. 6: A multisegmented presentation of a single-line mooring.

EXAMPLES

Multisegment, Single-Line System

An example of a single, homogeneous cable suspended between two points is considered. The line has the following properties:

- $EA = 9.817 \times 10^{10}$ N
- $L = 500$ m
- $l = 325$ m
- $h = -350$ m
- $W = 292.8$ N/m

Because the cable is freely hanging between two points, Eqs. 3a∼3b are simultaneously solved to find the fairlead forces H and V. The exact solution for a single-line suspended between the two points l and h amounts to $H = 615,677$ N and $V = 1,505,124$ N by solving the two equations simultaneously.

To check against MSQS model's accuracy, an identical line is assembled in MAP, except it is implemented as a multisegmented system with nine elements connected in series. The first element in the mooring line is suspended at $[l\ ,\ 0\ ,\ -h]^T$, and the last element at $[0\ ,\ 0\ ,\ 0]^T$, with sum lengths of all elements equal to 500 meters. The profile generated by MAP is pictured in Fig. 6, where each circular point along the line identifies a node. The fairlead force at the upper element is recorded as $H_9 = 615,456$ N and $V_9 = 1,504,890$ N, which agrees with the exact solution handled using Eqs. 3a∼3b. The fairlead tension found with MSQS line are within 0.035% of the exact analytical solution for a single-line.

MAP can output the fairlead tension along the line $T_e(s)$ as well as the fairlead force in XYZ global coordinates. As a further check, the researchers compared $T_e(s)$ for the single-line system with the horizontal H and vertical V force on all elements for the discretized system in Fig. 6. As shown in Fig. 5, the X and Z fairlead forces are written to the MAP summary text file by raising the `x_force` and `z_force` element flag. A summary of these findings is presented in Table 1 and agrees with the single-line analytical solution.

An Elaborate Multiline System

A more elaborate example is considered in this next numerical exercise. This case is devised to incorporate several elements strung between other cables, including one node upheld in the water column by a buoyancy tank with 100 m^3 of displaced volume. The system profile achieved at convergence is illustrated in Fig. 7. This example is particularly challenging to solve from a numerical computation perspective because the combination of equations needing to be simultaneously solved all have different orders of magnitude. This compels the Jacobian matrix to be 1) nonsymmetric and 2) to approach singularity. In particular, the ensemble of lines extending beyond their unstretched length L (elements 2, 3, 5, and 6), elements in contact with the seabed (elements 1, 4, and 9), and elements forming a classic catenary profile (elements 7 and 8), speak to this difficulty. By selecting appropriate solver options – in this case, a trust region nonlinear solver and the generalized minimal residual method (GMRES) iterative technique (Saad and Schultz, 1986) – the solution is found quickly. The input file used to generate the profile is shown in Fig. 8.

Table 1: Comparison of line tensions along a single-line element compared to the multisegmented presented in Fig. 6. The solution for $T_e(s)$ is the exact solution derived analytically for a single-line using Eq. 4. The magnitude of the vertical and horizontal fairlead force for the multisegmented system is calculated to find the equivalent mooring line tension T_e.

Element	$T_e(s)$, [N] (exact solution)	$\|H_i + V_i\|$, [N] (multisegmented solution)	% Difference
1, $s = 55.55$	$655,966$	$655,673$	0.045
2, $s = 111.10$	$726,777$	$726,449$	0.045
3, $s = 166.65$	$822,934$	$822,582$	0.043
4, $s = 222.20$	$936,663$	$936,294$	0.039
5, $s = 277.75$	$1,062,335$	$1,061,952$	0.036
6, $s = 333.30$	$1,196,193$	$1,195,797$	0.033
7, $s = 388.85$	$1,335,778$	$1,335,370$	0.031
8, $s = 444.40$	$1,479,469$	$1,479,048$	0.028
9, $s = 500.00$	$1,626,178$	$1,625,879$	0.018

To verify the mooring array profile generated by MAP, the forces on each individual mooring line are solved using Eqs. 3a∼3b and Eqs. 8a∼8b. That is, H and V are solved for one line alone based on the element l and h displacements as determined by MAP. A summary of the results delivered by MAP are shown in Table 2, and it agrees with the more precise single-line analytical solution. Because the mooring line is symmetric about the XZ plane at $Y = -50$ m, some elements share the same forces. As a further check, the sum forces on node nine can be verified by equating it with the user-defined buoyancy:

$$V_9 + V_7 + V_8 = \rho g B \tag{18}$$

The node buoyancy is:

$$\rho g B = 1025 \times 9.81 \times 100 = 1,005,525 \text{ N} \tag{19}$$

The difference between the left-hand side and right-hand side of Eq. 18 amounts to 2 N. Similarly, the sum forces for nodes 2 and 6 can be solved to check if the total force sums to zero. The vertical anchor force in element 7 is $V_{A_7} = 171458$ N. For elements 2 and 3:

- $V_{A_2} = 950707$ N
- $V_{A_3} = 290128$ N

$$V_1 + V_{A_2} - V_{A_3} - V_{A_7} = 0 \text{ N} \tag{20}$$

Symmetry rules that dictate results in Eq. 20 are identical for node 6.

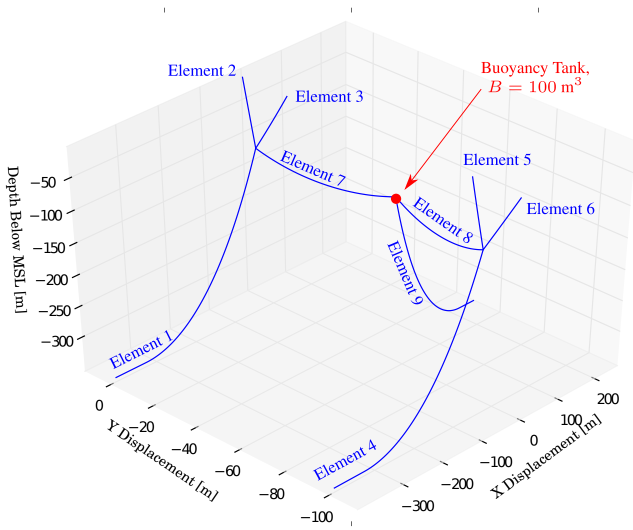

Fig. 7: An example of an elaborate system demonstrating MAP's ability to handle generic geometries.

```
--------------- LINE DICTIONARY -------------------
LineType  Diam   RhoInAir    E        CB
(-)       (m)    (kg/m^3)   (N/m^2)   (-)
steel     0.25   6500       200E9     1.0
nylon     0.35   1400       14E9      1.0
--------------- NODE PROPERTIES ------------------
Node Type       X      Y      Z    M     B      FX   FY   FZ
(-)   (-)      (m)    (m)    (m)  (kg)  (m^3)  (N)  (N)  (N)
1    fix      -400    0     -350  0     0       #    #    #
2    Connect #-90    #0    #-80   0     0       0    0    0
3    vessel   -10    10    -10    0     0       #    #    #
4    vessel   -10   -10    -10    0     0       #    #    #
5    fix      -400  -100   -350   0     0       #    #    #
6    Connect #-90  #-100   #-80   0     0       0    0    0
7    vessel   -10   -90    -10    0     0       #    #    #
8    vessel   -10   -110   -10    0     0       #    #    #
9    connect #-90  #-55    #-80   0     100     0    0    0
10   fix       250  -50    -350   0     0       #    #    #
--------------- LINE PROPERTIES ------------------
Element LineType UnstrLen NodeAnch NodeFair Flags
(-)      (-)      (m)       (-)      (-)     (-)
1        steel    480       1        2       plot
2        nylon    90        2        3       plot
3        nylon    90        2        4       plot
4        steel    480       5        6       plot
5        nylon    90        6        7       plot
6        nylon    90        6        8       plot
7        steel    100       2        9       plot
8        steel    100       9        6       plot
9        steel    350       10       9       plot
--------------- SOLVER OPTIONS--------------------
Option
(-)
-snes_type tr
-pc_type svd
-ksp_type gmres
```

Fig. 8: MAP input file for the profile pictured in Fig. 7.

Table 2: Comparison of line tensions along each single-line element as pictured in Fig. 7. The solution for $T_e(s)$ is the exact solution derived analytically from Eq. 4. The magnitude of the vertical and horizontal fairlead force for the multisegmented system must be calculated to find the equivalent mooring line tension T_e.

Element	l	h	H & V MAP Solution	H & V Eqs. 3a∼3b or Eqs. 8a∼8a
1/4	363.27	254.60	$H = 516,315$ $V = 1,069,377$	$H = 516,309$ $V = 1,069,374$
2/6	28.61	85.40	$H = 323,831$ $V = 982,562$	$H = 324,002$ $V = 983,063$
3/5	28.46	85.40	$H = 101,892$ $V = 321,982$	$H = 102,376$ $V = 323,425$
7/8	88.02	-20.13	$H = 143,286$ $V = 92,188$	$H = 143,282$ $V = 92,190$
9	211.13	234.47	$H = 236,345$ $V = 821,147$	$H = 219,487$ $V = 808,359$

CONCLUSION

This paper defines the theory used in assembling the Mooring Analysis Program's (MAP's) multisegmented, quasi-static (MSQS) solver. The structure of the nonlinear equations being solved is based on the earlier work presented by Peyrot and Goulois (1979). The new framework created in this paper differs from other works in that: 1) a closed-form analytical solution for a cable touching the seabed has been implemented, 2) the MSQS package is integrated with the Portable, Extensible Toolkit for Scientific Computation (PETSc) numerical library to better handle ill-conditioned problems, and 3) the model avoids *a priori* assumptions regarding the known boundary conditions or model geometry, thereby allowing generic problems to be solved. MAP was developed adhering to NREL's FAST program framework to allow a varying degree of modeling fidelity and code coupling options. In addition, MAP is callable in Python; however, this paper does not demonstrate this feature. Refer to Masciola and Jonkman (forthcoming) for a more in-depth treatment of the MSQS usage.

Through the creation of the MSQS solver, the groundwork was formed to develop a finite-element component to MAP to model cable dynamics. The premise taken in developing this tool was to fully develop the MSQS using the essential building blocks (such as nodes and elements) needed for a finite-element analysis (FEA) cable program. Once the MAP program interface is defined, the FEA component to MAP can be developed by modifying the program data structure definitions in the MSQS module. Built from the requirements of an FEA model, the MSQS model also requires nodes and elements to form the cable geometry, boundary conditions, and restoring forces. The primary difference between the MSQS model and an FEA solution are: 1) the forces operating on the nodes, and 2) the FEA models have differential equations that need to be integrated.

ACKNOWLEDGMENT

This research was funded by the U.S. Department of Energy's Wind and Water Power Program.

REFERENCES

API Recommended Practice 2T (1997). *Recommended Practices for Planning, Designing, and Constructing Tension Leg Platforms*, American Petroleum Institute, 254 pp.

Balay, S, Brown, J, Buschelman, K, Eijkhout V, Gropp, WD, Kaushik, D, Knepley, MG, Curfman McInnes, L, Smith, BF, and Zhang, H, (2012). *PETSc Users Manual*, Argonne National Laboratory, ANL-95/11 - Revision 3.3.

Faires, JD, and Burden, R, (2003). *Numerical Methods, 3^{rd} Edition*, Brooks/Cole-Thomson Learning, Pacific Grove, CA, 622 pp.

Irvine, M (1992). *Cable Structures*. Dover Publications, 272 pp.

Jonkman, JM, and Buhl Jr., ML (2005). *FAST User's Guide*, NREL Technical Report, NREL/EL-500-29798.

Jonkman, JM (2007). *Dynamics Modeling and Loads Analysis of an Offshore Floating Wind Turbine*. The National Renewable Energy Laboratory, Technical Report NREL/TP-500-41958, 233 pp.

Jonkman, JM, (2013). "The New Modularization Framework for the FAST Wind Turbine CASE Tool," 32^{nd} ASME Wind Energy Symposium, January 7-10, Grapevine, Texas, USA.

Kozak, K, Zhou, W, and Jinsong, W (2006). "Static Analysis of Cable-Drive Manipulators with Non-Negligible Cable Mass," *IEEE Transactions on Robotics*, Vol 22, No. 3, pp. 425-433.

Langtangen, HP (2011). *A Primer on Scientific Programming with Python, 2^{nd} Edition*, Springer Verlag, New York, NY, USA, pp. 798.

Masciola, MD, and Jonkman, J, (forthcoming). *The MAP User Guide (DRAFT)*, NREL Technical Report, Golden, CO.

Paul, B and Soler, A (1995). "Cable Dynamics and Optimum Towing Strategies for Submersibles," *The 15th Annual Offshore Technology Conference*, Houston, TX, pp. 507-513.

Peyrot, AH, and Goulois, AM (1979). "Analysis of Cable Structures," *Computers & Structures*, Vol 10, pp. 805-813.

Saad, Y, and Schultz, MH, (1986). "Gmres: A Generalized Minimal Residual Algorithm for Solving Nonsymmetric Linear Systems," *SIAM Journal on Scientific Computing*, No. 7, pp. 856-869.

Wang, L, Guo, Z, and Yuan, F (2010). "Quasi-Static Three-Dimensional Analysis of Suction Anchor Mooring System," *Ocean Engineering*, No. 37, pp. 1127-1138.

Wilson, JM (2003). *Dynamics of Offshore Structures*, John Wiley & Sons, pp. 325.